

1 **TITLE:** The Type VI secretion system of *Stenotrophomonas rhizophila* CFBP13503 limits the
2 transmission of *Xanthomonas campestris* pv. *campestris* 8004 from radish seeds to seedlings

3

4 **AUTHORS :** Tiffany Garin¹, Chrystelle Brin¹, Anne Préveaux¹, Agathe Brault¹, Martial
5 Briand¹, Marie Simonin¹, Matthieu Barret¹, Laure Journet², Alain Sarniguet¹

6

7 ¹ Univ Angers, Institut Agro, INRAE, IRHS, SFR QUASAV, F-49000 Angers, France

8 ² Laboratoire d'Ingénierie des Systèmes Macromoléculaires, Institut de Microbiologie,
9 Bioénergies et Biotechnologie, Institut de Microbiologie de la Méditerranée, Aix-Marseille
10 Université-CNRS, UMR 7255, Marseille, France

11

12 **Corresponding author:** Alain Sarniguet, alain.sarniguet@inrae.fr

13

14 **Keywords:** Type VI Secretion System, interbacterial competition, seed, seedling transmission,
15 *Stenotrophomas rhizophila*, *Xanthomonas campestris* pv. *campestris*.

16

17 **ABSTRACT**

18 *Stenotrophomonas rhizophila* CFBP13503 is a seed-borne commensal bacterial strain, which
19 is efficiently transmitted to seedlings and can outcompete the phytopathogenic bacteria
20 *Xanthomonas campestris* pv. *campestris* (Xcc8004). The type VI Secretion System (T6SS), an
21 interference contact-dependent mechanism, is a critical component of interbacterial
22 competition. The involvement of the T6SS of *S. rhizophila* CFBP13503 in the inhibition of
23 Xcc8004 growth and seed-to-seedling transmission was assessed. The T6SS cluster of *S.*
24 *rhizophila* CFBP13503 and nine putative effectors were identified. Deletion of two T6SS
25 structural genes, *hcp* and *tssB*, abolished the competitive advantage of *S. rhizophila* against
26 Xcc8004 *in vitro*. The population sizes of these two bacterial species were monitored in
27 seedlings after inoculation of radish seeds with mixtures of Xcc8004 and either *S. rhizophila*
28 wild type (wt) strain or isogenic *hcp* mutant. A significant decrease in the population size of
29 Xcc8004 was observed during confrontation with the *S. rhizophila* wt in comparison to T6SS-
30 deletion mutants in germinated seeds and seedlings. We found that the T6SS distribution among
31 835 genomes of the *Stenotrophomonas* genus is scarce. In contrast, in all available *S. rhizophila*
32 genomes, T6SS clusters are widespread and mainly belong to the T6SS group i4. In conclusion,
33 the T6SS of *S. rhizophila* CFBP13503 is involved in the antibiosis against Xcc8004 and reduces
34 seedling transmission of Xcc8004 in radish. The distribution of this T6SS cluster in the *S.*
35 *rhizophila* complex could make it possible to exploit these strains as biocontrol agents against
36 *X. campestris* pv. *campestris*.

37

38 1 - INTRODUCTION

39 Disease emergence of plant pathogens is the result of changes in host range and/or
40 pathogen dispersion into a new geographic area (Engering et al., 2013). Regarding this second
41 point, seed transmission represents an important means of pathogen dispersion and is therefore
42 significant in the emergence of plant diseases (Baker and Smith, 1966). Indeed, the International
43 Seed Testing Association Reference Pest List v9 identified 333 seed-borne pests (viruses,
44 bacteria, fungi, oomycetes and nematodes) in more than 50 plant species (Denancé and
45 Grimault, 2022). Of these seed-borne pests 145 are directly transmitted to plants (Denancé and
46 Grimault, 2022).

47 Pathogens are not the only microorganisms that can be carried by seeds. More than
48 1,000 bacterial and fungal taxa were identified in the seed microbiota of 50 plant species
49 (Simonin et al., 2022). This important microbial diversity observed on seed samples is however
50 more restricted at the scale of an individual seed with one dominant taxon of variable identity
51 (Chesneau et al., 2022; Newcombe et al., 2018). Since the seed is a limited habitat in terms of
52 resources and space, microbial competition is likely to play an important role in seed microbiota
53 assembly. Using these competition processes to promote seed transmission of non-pathogenic
54 microorganisms at the expense of plant pathogens could be deployed as a biocontrol-based
55 strategy (Barret et al., 2016). However, this approach requires a better understanding of the
56 mechanisms involved in these microbial competition processes, notably the relative importance
57 of exploitative competition (i.e. increase uptake and use of nutrients) versus interference
58 competition (i.e. limiting the access of other cells to resources, Granato et al., 2019).

59 The *Lysobacteraceae* (earlier known as *Xanthomonadaceae*) family includes numerous
60 species of plant pathogens like *Xanthomonas* spp. (Jacques et al., 2016) and also ubiquitous
61 *Stenotrophomonas* spp. like commensal *S. rhizophila* (Wolf et al., 2002) and opportunistic
62 human pathogens like *S. maltophilia* (Gröschel et al., 2020). *X. campestris* pv. *campestris*
63 (Xcc), the causal agent of black rot disease of *Brassicaceae* (Vicente and Holub, 2013) is not
64 only seed-transmitted in a range of *Brassicaceae* (Randhawa, 1984; Rezki et al., 2016; van der
65 Wolf et al., 2019) but also in non-host plants such as common bean (Darrasse et al., 2010).
66 Diversity surveys of the radish seed microbiota have highlighted that Xcc shares the same
67 habitat as numerous bacterial strains related to the *S. rhizophila* species (Rezki et al., 2016,
68 2018). Strains of *S. rhizophila* are efficient seedling colonizers of cotton, tomato, sweet pepper
69 (Schmidt et al., 2012) and radish (Simonin et al., 2023) as well as commonly isolated in the
70 rhizosphere of different plant species including rapeseed (Berg et al., 1996) and potato
71 (Lottmann et al., 1999). The type strain of *S. rhizophila*, DSM14405^T, can protect plants against
72 osmotic stress (Alavi et al., 2013; Egamberdieva et al., 2011) and limits the growth of fungal
73 pathogens (Minkwitz and Berg, 2001). Other strains of *S. rhizophila* possess antibacterial
74 activities (Lottmann et al., 1999). For instance, the strain *S. rhizophila* CFBP13503 decreases
75 the population size of Xcc during *in vitro* confrontation assays (Torres-Cortés et al., 2019). This
76 decrease in Xcc population size was attributed to exploitative competition since these strains
77 shared significant overlaps in resource utilization (Torres-Cortés et al., 2019). However, the
78 role of interference competition was only partially assessed through the production of diffusible
79 molecules, while contact-dependent mechanisms were not tested.

80 Among the contact-dependent mechanisms involved in interbacterial competition, the
81 type VI secretion system (T6SS) is probably the most widely distributed with more than 17,000
82 T6SS gene clusters distributed in more than 8,000 genomes sequences (source SecReT6 v3,
83 Zhang et al., 2022). T6SS is a multi-protein complex composed of several core components,
84 including the membrane complex TssJLM, the baseplate TssEFGK, the tail tube Hcp (TssD),
85 the spike composed of VgrG (TssI) trimers topped by a protein containing a Pro-Ala-Ala-Arg
86 Repeat (PAAR) motif, the contractile sheath TssBC, and the coordinating protein TssA, as well
87 as the sheath disassembly ATPase ClpV (also known as TssH) (Cherrak et al., 2019; Cianfanelli
88 et al., 2016; Ho et al., 2014). The T6SS allows bacteria to compete and survive in their
89 environments by injecting toxins/effectors into target cells. Effectors are either fused
90 ("specialized" effectors) to or interact ("cargo" effectors) with Hcp tube or VgrG/PAAR spike
91 proteins (Cherrak et al., 2019; Cianfanelli et al., 2016; Jurénas and Journet, 2021). The
92 contraction of the sheath leads to the injection of Hcp and VgrG/PAAR proteins together with
93 the effectors. Effector-immunity encoding gene pairs are often associated with genes encoding
94 the elements involved in their delivery. These include Hcp, VgrG or PAAR proteins, and also
95 accessory proteins named chaperones/adaptors, which facilitate the loading of effectors onto
96 the T6SS elements (Unterweger et al., 2017). Adaptors identified so far are DUF4123,
97 DUF1795, DUF2169, and DUF2875-containing proteins encoded upstream of their cognate
98 effector (Berni et al., 2019; Unterweger et al., 2017). If effector-immunity can be orphan genes,
99 they are often encoded in T6SS clusters or associated with *hcp* or *vgrG* in orphan *hcp/vgrG*
100 islands. Conserved domains or motifs have also been described for some effectors and
101 immunity proteins which facilitate their identification (Lien and Lai, 2017). For effector
102 proteins, these conserved domains can reflect their biochemical toxic activity. Recruitment
103 domains and motifs, such as MIX (Marker for type sIX effectors) or FIX (Found in type sIX
104 effectors) motifs, DUF2345/TTR (Transthyretin-like domains) domains or Rhs (Rearrangement
105 hot spot) domains can be found in T6SS effectors and are related to their mode of delivery
106 (Cianfanelli et al., 2016; Cherrak et al., 2019; Jurénas and Journet, 2021).

107 Type VI secretion system is widespread among plant-associated bacteria and divided
108 into five taxonomic groups (Bernal et al., 2018). T6SS has been implicated in a wide range of
109 biological processes, including microbial competition with bacteria and fungi (Luo et al., 2023;
110 Trunk et al., 2018), epiphytic colonization of bacterial pathogens (Liyanapathirana et al.,
111 2021), and pathogen virulence (Choi et al., 2020; Montenegro Benavides et al., 2021; Shyntum
112 et al., 2015). *Pseudomonas putida* KT2440 K1-T6SS also provides biocontrol properties by
113 killing *X. campestris* when injected into plant leaves (Bernal et al., 2017). Commensal bacteria
114 from seed microbiota carrying T6SS could be good candidates as biocontrol agents and may be
115 used to limit bacterial pathogen transmission from seed to seedling. In the course of this work,
116 we explored the possibility of limiting Xcc transmission from seed to seedling through a
117 contact-dependent T6SS mechanism mediated by *S. rhizophila*. We also ask to which extent
118 strains from the *Stenotrophomonas* genus share similar or different T6SS clusters.

119

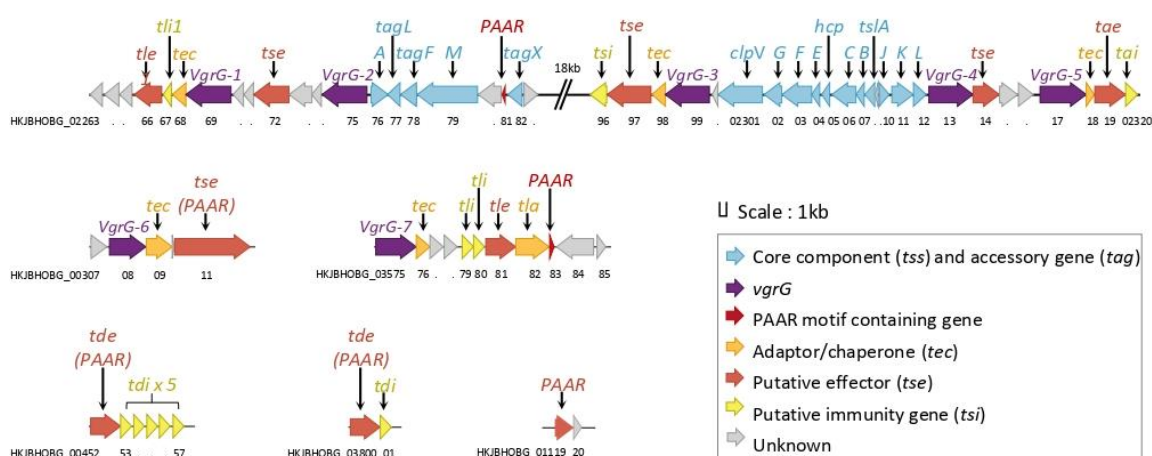
120 **2 - RESULTS**

121 **Genomic organization of *S. rhizophila* CFBP13503 T6SS**

122 Fourteen genes encoding T6SS core protein components were identified in the genome
123 sequence of *S. rhizophila* CFBP13503 (**Figure 1**). These genes, located on a single genomic
124 cluster of 72 kb, include genes encoding proteins involved in the membrane complex (TssJ, L
125 and M: HKJBHOBG_02310, 02312, 02279), the baseplate (TssE, F, G and K: HKJBHOBG_02304,
126 02303, 02302, 02311), the contractile sheath (TssB and C: HKJBHOBG_02307, 02306), the
127 coordinating protein (TssA: HKJBHOBG_02276), the disassembly ATPase (TssH: HKJBHOBG_02301),
128 the inner tube (Hcp: HKJBHOBG_02305) and the puncturing structure (VgrG and PAAR). Regarding the
129 puncturing structure, multiple genes encoding VgrG (n=7) and PAAR domain-containing
130 proteins (n=5) were detected in the genome sequence.

132 Based on the genetic architecture of the T6SS genomic cluster, the T6SS is related to group i4
133 (Bayer-Santos et al., 2019). T6SS putative accessory genes were identified in the core structural
134 cluster, including the group 4-specific : *i*) the group 4-specific *tagX* (HKJBHOBG_02282),
135 which encodes an L,D-endopeptidase first proposed to be involved in cell wall degradation for
136 T6SS assembly (Weber et al., 2016), but essential for polymerisation of the contractile sheath
137 and not required for assembly of the membrane complex and the baseplate (Lin et al., 2022),
138 *ii*) *tagF* (HKJBHOBG_02278), which encodes a negative post-translational regulator of the *P.*
139 *aeruginosa* H1-T6SS (Lin et al., 2018), *iii*) *tagN/L* (HKJBHOBG_02277), whose role in T6SS
140 assembly or regulation remains unknown and *iv*) *tslA* (HKJBHOBG_02308), conserved in i4b
141 T6SS and involved in cell-contact T6SS assembly (Lin et al., 2022).

142



143

144 **Figure 1. *S. rhizophila* CFBP13503 T6SS genomic architecture.** Schematic representation
145 of *S. rhizophila* CFBP13503 T6SS cluster along with orphan *vgrG* and PAAR clusters. Genes
146 are coloured according to their functional roles: core component and accessory genes (blue),
147 *vgrG* (violet), PAAR-motif containing genes (red), adaptor/chaperone (orange), putative
148 effector (orange-red), immunity genes (yellow), and genes with unknown function (grey).

149 **The T6SS of *S. rhizophila* CFBP13503 encodes a wealth of putative effectors**

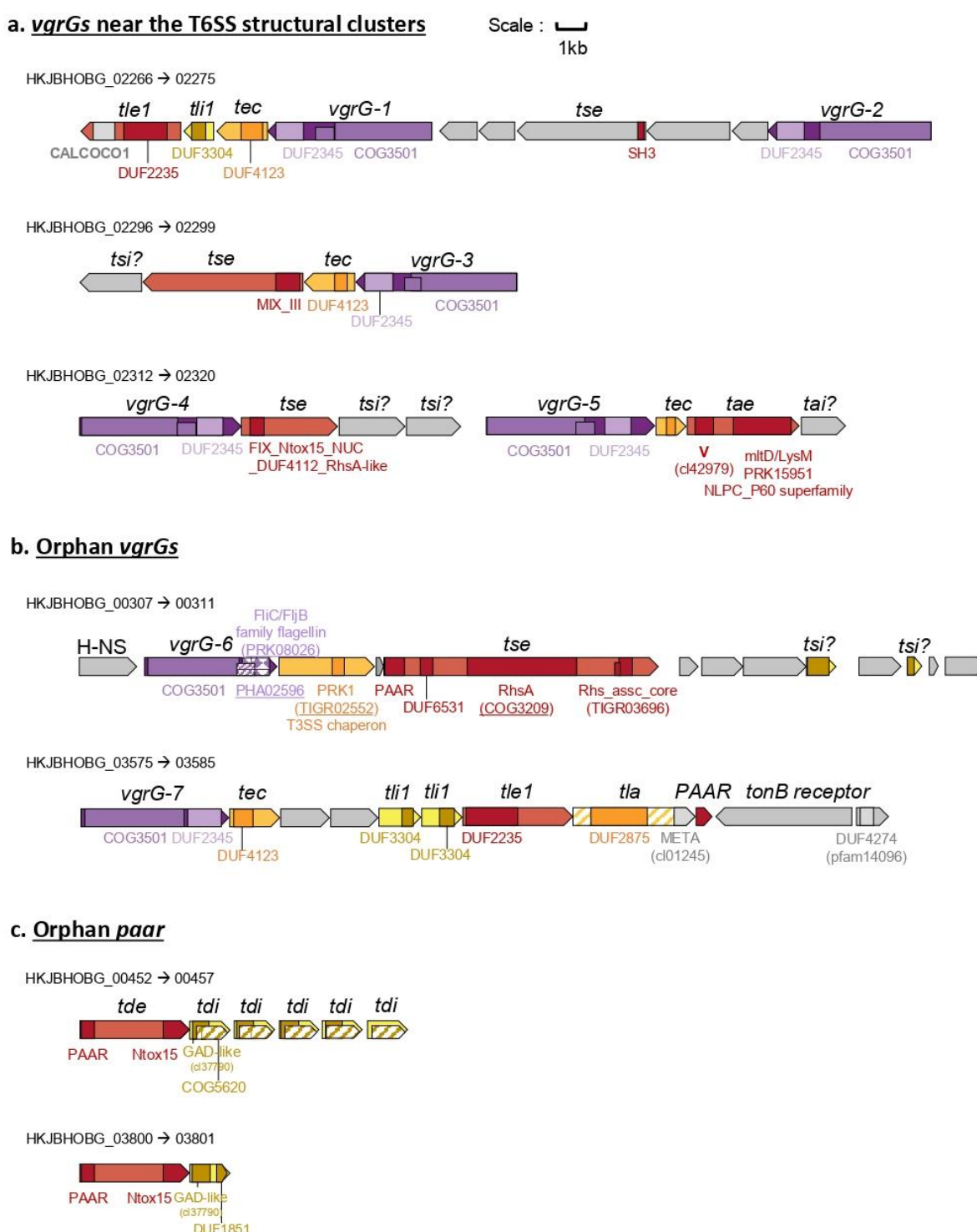
150 To identify putative T6SS effectors of CFBP13503, we screened the T6SS main cluster and the
151 *vgrG* and PAAR islands for the presence of "specialized" VgrG, Hcp, or PAAR proteins, as
152 well as the presence of N-terminal effectors motifs such as FIX or MIX domains. We also
153 looked for conserved domains encoded by the genes in the vicinity of *vgrG*, *hcp* or *PAAR* or
154 adaptor/chaperones that could be cargo effectors associated with immunity proteins.

155 We identified only one Hcp protein, encoded in the main T6SS cluster in between *tssE* and *tssC*
156 genes. Seven *vgrG* genes (*vgrG-1* to *vgrG-7*) were identified, with five of them located adjacent
157 to the T6SS cluster and two others scattered throughout the genome (**Figures 2a and 2b**). All
158 VgrG proteins, except VgrG-6, contain a C-terminal DUF2345 domain extending the VgrG
159 needle that can be important for recruiting effectors or carrying toxic activity (Flaughnatti et al.,
160 2016, 2020; Storey et al., 2020). In contrast, VgrG-6 contains a C-terminal domain extension
161 with a weak (*p*-value = 5.52e-03) similarity to the FliC/FljB family flagellin (accession:
162 cl35635). Five PAAR-containing proteins were detected in the genome of CFBP13503: one in
163 the T6SS cluster, one in each *vgrG* island and two orphans PAAR proteins (**Figure 2**). The
164 latter two PAAR-containing proteins possess a C-terminal Ntox15 domain (pfam15604) with a
165 HxxD catalytic motif. Such domains were found associated with T6SS effectors with DNase
166 activity called Tde (Type VI DNase effector) (Ma et al, 2014; Luo et al 2023). These two
167 predicted PAAR-fused Tde proteins are associated with genes encoding the DUF1851 domain,
168 known to be associated with T6SS Tde immunity proteins (Tdi) (Ma et al, 2014; Luo et al 2023)
169 (**Figure 2c**).

170 In addition to "specialized" effectors, we detected several putative "cargo" effectors, immunity
171 proteins and chaperone proteins. Regarding chaperones, three DUF4123 domain-containing
172 proteins were identified in CDS located immediately downstream of *vgrG-1*, *vgrG-3* and *vgrG-7*. Another chaperone containing a DUF2875 domain was also encoded in the vicinity of *vgrG-7*. Concerning effector, two effector-immunity (E-I) encoding gene pairs *tle/tli* were associated
173 with VgrG-1 and VgrG-7. Both *tle* encode proteins containing a GXSXG motif (GFSRG) and
174 a DUF2235, characteristic of the T6SS phospholipase effector (Tle) of the Tle1 family.
175 (Flaughnatti et al., 2016; Russell et al., 2013). Their corresponding Tli contained a DUF3304
176 domain found in several T6SS Tli1 immunity proteins (Russell et al., 2013). A putative
177 amidase effector, *tae*, was associated with VgrG-5. This effector contained a murein
178 transglycosylase D domain and a LysM motif involved in binding peptidoglycan, as well as an
179 NlpC_P60 domain. Linked to the other *vgrG* genes, we also detected genes encoding T6SS
180 effectors specific domains MIX and FIX. The MIX-containing effector located at the vicinity
181 of *vgrG-3* and a tec protein-encoding gene may encode a pore-forming toxin. This toxin is
182 predicted to encode 4-5 putative transmembrane domains at its C-terminus. A predicted
183 structure-based search using AlphaFold2 predicted structure and Foldseek suggest that this
184 protein shares structural homologies (over the 900 first residues) with VasX, a pore-forming
185 toxin from *Vibrio cholerae* (Miyata et al., 2013). The downstream gene is a predicted inner
186 membrane protein and could be the corresponding immunity protein. Unfortunately, we were
187 unable to determine conserved domains or potential activities for the FIX-containing protein
188 encoded downstream *vgrG-4* so we referred to it as *tse*, which stands for "type six effector".
189
190

191 Similarly, no function could be assigned to the proteins encoded by the genes downstream *vgrg-*
192 *4*. We assume that these genes could encode potential toxins and associated immunity proteins
193 and potential chaperones. The 18kb inter region between *tssM* and *tssA* and other structural
194 genes contains a poly-immunity locus with a predicted formylglycine-generating enzyme
195 family immunity protein encoding gene (Lopez et al. 2021) and 8 duplications of the putative
196 immunity gene HKJBHOBG_02263 containing a DUF6708 domain.

197



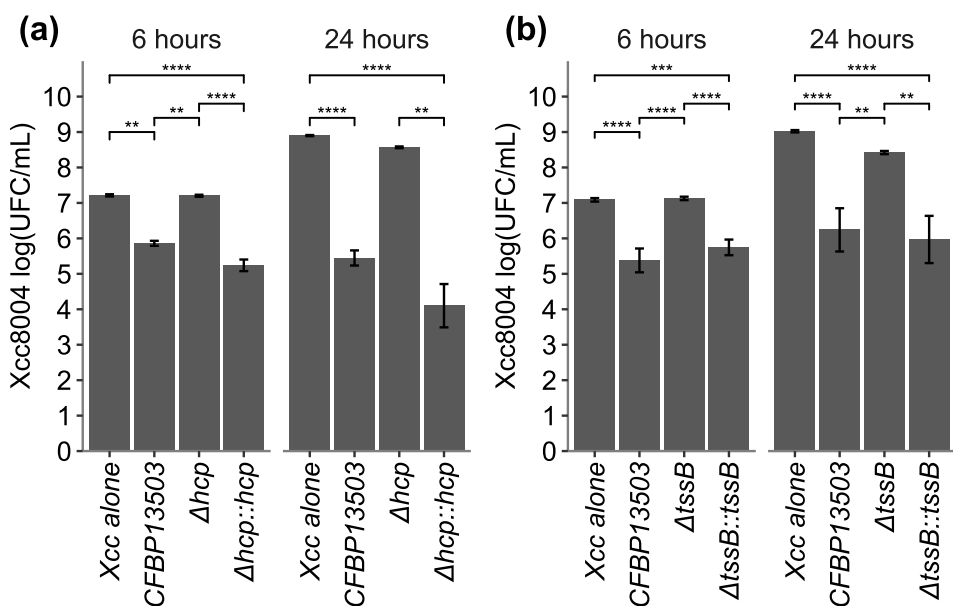
198

199 **Figure 2. *S. rhizophila* CFBP13503 T6SS effectors.** The conserved domain organization of
200 genes encoding putative chaperone, effector and immunity proteins associated with (a) VgrG
201 encoded in the main T6SS cluster, (b) orphan VgrG, and (c) orphan PAAR domain-containing
202 effectors are represented. VgrG genes are indicated in violet, putative effectors with or without
203 PAAR motif are shown in red, chaperone genes in orange, immunity protein genes in yellow
204 and gene-encoded proteins with unknown functions are in grey.

205 ***S. rhizophila* CFBP13503 outcompete Xcc8004 *in vitro* in a T6SS-dependent manner**

206 *Stenotrophomonas rhizophila* CFBP13503 is able to outcompete the phytopathogenic bacterial
207 strain Xcc8004 in TSB10 (Torres-Cortés et al., 2019). After 6 hours of confrontation on TSA10
208 medium between Xcc8004 and CFBP13503, a 10 to 100-fold decrease in Xcc8004 population
209 was observed in comparison to Xcc8004 monoculture (Figure 3). Deletion of two genes
210 encoding proteins involved in T6SS assembly (Δhcp and $\Delta tssB$) significantly increased the
211 population size of Xcc8004 to a level comparable to Xcc8004 monoculture (Figure 3).
212 Complementation of these two mutants restored the decrease in CFU of Xcc8004. These results
213 demonstrate that the T6SS of *S. rhizophila* CFBP13503 is involved in the antibiosis towards
214 Xcc8004 from 6 hours of confrontation. T6SS effect size increased with time as 24 hours after
215 confrontation Xcc8004 population decreased from 1,000 to 10,000 times in the wild-type strain
216 and complemented mutants. At 48h the Xcc populations were reduced by the wild type
217 compared to the deletion mutants but increased by one log10 compared to the same wild type
218 treatment at 6 and 24 h (Fig. S3). These results highlight the involvement of the T6SS of *S.*
219 *rhizophila* CFBP13503 in the killing of Xcc8004 and thus its involvement in interbacterial
220 competitions.

221



222

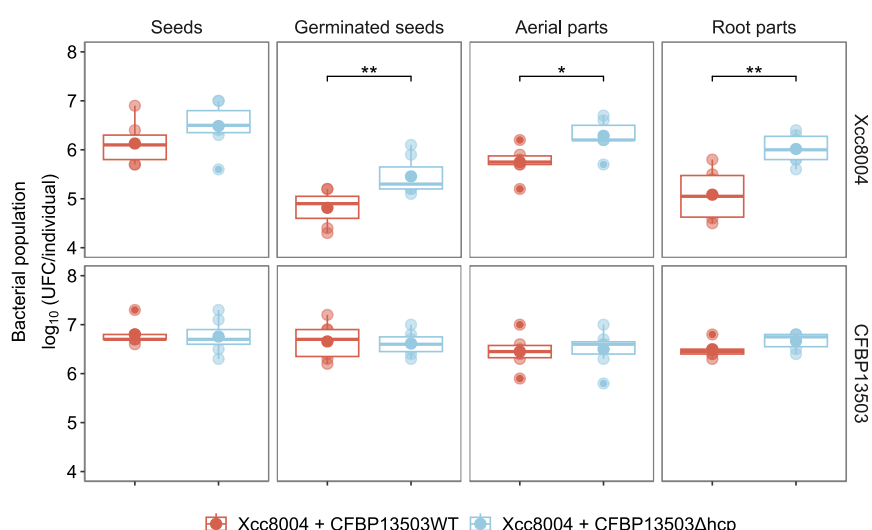
223 **Figure 3. Bactericidal activity of *S. rhizophila* CFBP13503 against *X. campestris* pv.
224 *campestris* 8004.** Confrontation between Xcc8004 and i) *S. rhizophila* CFBP13503 wild-type,
225 ii) T6SS-deficient mutants Δhcp (a) and $\Delta tssB$ (b) and iii) the complemented mutants $\Delta hcp::hcp$
226 and $\Delta tssB::tssB$ in TSA10 medium for 6h and 24h. Colony-forming units (CFU) were
227 quantified on TSA10 supplemented with rifampicin. The averages \pm sd of 9 replicates are
228 plotted. Statistical analyses were performed using Dunn's Multiple Comparison Test (* p-value
229 < 0,05; ** p-value <0,005; *** p-value < 0,0005; **** p-value < 0,00005).

230

231 **The T6SS of *S. rhizophila* CFBP13503 limits the seed-to-seedling transmission of Xcc8004
232 in radish.**

233 To investigate the bactericidal impact of CFBP13503 T6SS *in planta*, seedling transmission
234 assays were carried out on radish seeds (**Figure 4**). Xcc8004 was co-inoculated with either the
235 wild-type CFBP13503 strain or the *Δhcp* mutant on sterilized seeds with inoculum ratios of
236 1:2.1 and 1:1.6 respectively. Hcp protein is a structural protein of T6SS syringe but could exert
237 antibiosis against bacterial preys (Decoin et al. 2014, Fei et al. 2022). Thus, we chose the *hcp* mutant
238 to prevent any toxicity. Bacterial population sizes were measured on seeds, germinated seeds (1
239 dpi) and the aerial and root parts of seedlings (5 dpi) by quantification of CFU on selective
240 media. The Xcc8004 population of inoculated seeds presented a variable (6.1 to 6.5
241 $\log_{10}(\text{UFC}/\text{sample})$) but no significant decrease when co-inoculated with wild-type CFBP13503
242 compared to the *Δhcp* mutant. However, a significant decrease in the Xcc8004 population was
243 observed from the germinated seed stage when co-inoculated with the wild-type strain. This
244 decrease persisted over time, with a significant reduction in Xcc8004 population size in the
245 aerial and root part of seedlings during the confrontation with the wild-type
246 CFBP13503 (**Figure 4**). The population size of *S. rhizophila* was not impacted by the presence
247 or absence of a functional T6SS (**Figure 4**). Altogether these findings show that the T6SS of *S.
248 rhizophila* CFBP13503 restricted seedling transmission of Xcc8004 without providing a fitness
249 advantage to *S. rhizophila* CFBP13503.

250



251

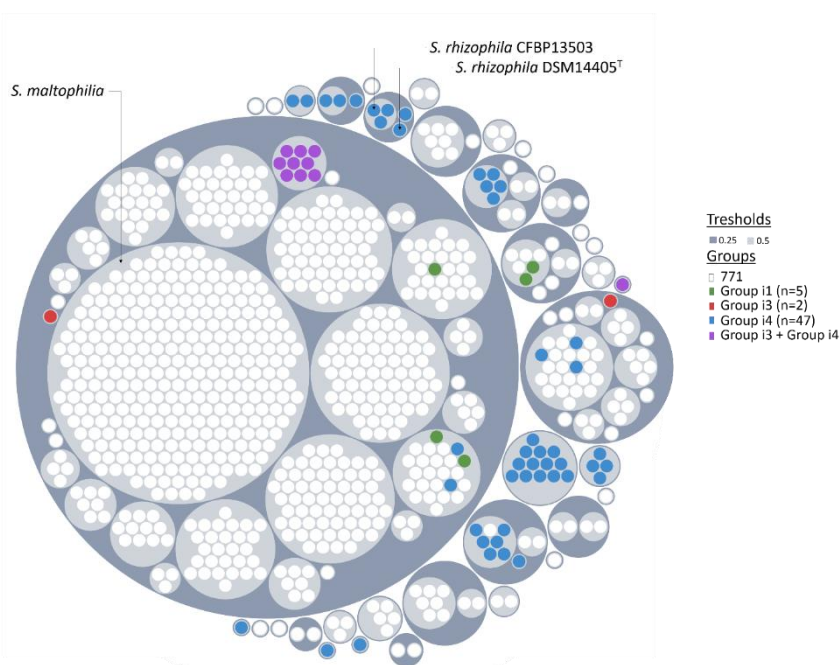
252 **Figure 4. Bacterial population dynamics during seed-to-seedling transmission of *S.
253 rhizophila* CFBP13503 and Xcc8004 in radish.** Radish seeds were co-inoculated with
254 Xcc8004 and (i) CFBP13503 wild-type or (ii) T6SS-deficient *Δhcp*. Bacterial populations were
255 assessed in radish seeds (0 dpi), 24-hour-old germinated seeds (1 dpi), 5-day-old seedling aerial
256 parts, and 5-day-old seedling root parts (5 dpi). Colony-forming units (CFU) were quantified
257 on selective media to differentiate Xcc8004 and CFBP13503 populations. The averages \pm sd of
258 two experiments (n=3 and n=4) are plotted. Statistical analyses were performed using Dunn's
259 Multiple Comparison Test (* p-value < 0,05; ** p-value <0,005).

260 **Analysis of T6SS distribution within the *Stenotrophomonas* genus**

261 Given the significant effect of *S. rhizophila* CFBP13503 T6SS on Xcc8004, it raises the
262 question of T6SS distribution within the *Stenotrophomonas* genus. A total of 835
263 *Stenotrophomonas* genome sequences were then collected from the NCBI (experimental
264 procedure). These genome sequences are divided into 95 groups (**Figure S1**) at a threshold of
265 50% shared 15-mers, an overall genome relatedness index employed as a proxy for species
266 delineation (Briand et al., 2021). From this analysis, the strain CFBP13503 is grouped with *S.*
267 *rhizophila* DSM14405^T in the same species complex (threshold 0.25) but differs from the
268 DSM14405^T type strain of *S. rhizophila* (threshold 0.5). So, we describe here a new *S.*
269 *rhizophila* complex.

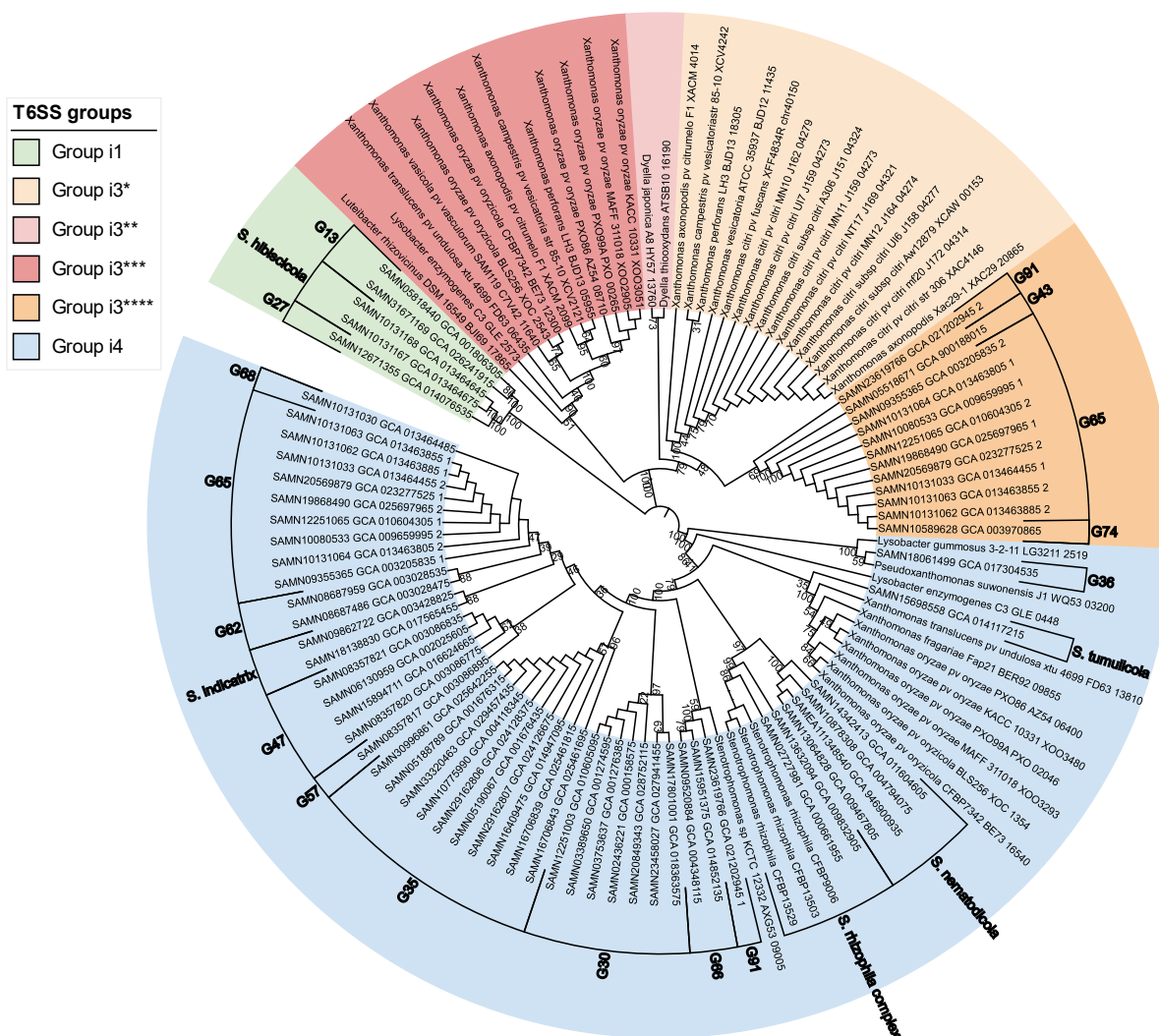
270 Sixty-four strains (8.3% of the dataset) of 22 groups contained at least one T6SS cluster (**Figure**
271 **5**). Based on the phylogenetic analysis of TSSC (**Figure 6**), T6SS clusters were classified into
272 three families i1 ($n=5$), i3 ($n=10$), and i4 ($n=57$). Just four species among the 28 groups of *S.*
273 *malophilia* species complex contain one T6SS except group 65 which contains two T6SS
274 belonging to two different taxonomic groups (i3 and i4). All *S. rhizophila* strains (**n=5**) have a
275 T6SS related to group i4.

276



277

278 **Figure 5. T6SS distribution among *Stenotrophomonas* sp..** Circle packing representation of
279 *Stenotrophomonas* sp. genomes ($n=835$). Overall genome relatedness was assessed by
280 comparing the percentage of shared 15-mers. Each dot represents a genome sequence, color-
281 coded based on the T6SS group. The genomes were grouped using two distinct thresholds to
282 assess species-specific relationships (0.5) and interspecies relationships (0.25). Interactive
283 circle packing representation is available in Figure S1. For the caption of species names when
284 a reference strain exists see Figure S2.



285

286 **Figure 6. T6SS distribution among *Lysobacteraceae*.** Phylogenetic tree based on TssC
287 protein sequences, constructed using a Kimura two-parameter neighbor-joining method with
288 1000 bootstrap replicates. The tree includes *Stenotrophomonas* and other *Lysobacteraceae*, as
289 studied by Bayer-Santos et al. in 2019. Strain taxonomic affiliation is based on KI-S grouping
290 (Figure S1).

291

292 **3- DISCUSSION**

293 *Xanthomonas campestris* pv. *campestris* is a frequent seed-colonizer of various host and non-
294 host plant species (Darrasse et al., 2010; Vicente and Holub, 2013). In the seed habitat, Xcc can
295 co-occur with other bacterial species such as *S. rhizophila* CFBP13503 (Rezki et al., 2016),
296 which can outcompete Xcc8004 *in vitro* (Torres-Cortés et al., 2019). Resource overlap was
297 initially proposed as the mode of action involved in Xcc8004 growth reduction in the presence
298 of *S. rhizophila* CFBP13503 (Torres-Cortés et al., 2019).

299 In this study, we showed that the growth inhibition of Xcc8004 by *S. rhizophila* CFBP13503
300 was T6SS-dependent. CFBP13503 decreased Xcc8004 population size from 10 to 1,000-fold
301 after 6h and 24h of confrontation in solid medium, respectively. Deletion mutants of two genes
302 encoding proteins (Δhcp and $\Delta tssB$) involved in T6SS assembly were no longer able to reduce
303 Xcc8004 growth. After 48h of confrontation *in vitro*, Xcc8004 strain partially escaped T6SS
304 antibiosis due to the possible establishment of non-immune defenses by Xcc such as the
305 creation of dead cell barriers or the production of exopolysaccharides that limit cell-to-cell
306 contact (Hersch et al., 2020). Antibacterial activities of T6SS can be contact-dependent with
307 the translocation of effector proteins in bacterial cells (Jurénas and Journet, 2021) or contact-
308 independent with the secretion of metal scavenging proteins in the surrounding media (Chen et
309 al., 2016; Lin et al., 2017; Si et al., 2017). When the confrontation between Xcc8004 and
310 CFBP13503 took place in a liquid medium with limited cell contacts, no difference in Xcc8004
311 growth was observed between the wild-type strain and the T6SS-deficient mutants (**Fig. S4**). In
312 conclusion, T6SS-mediated reduction in Xcc8004 growth is contact-dependent and therefore
313 due to the injection of protein effectors in Xcc8004 cells.

314 Furthermore, *S. rhizophila* CFBP13503 is involved in reducing the transmission of Xcc8004
315 from seed to seedling. When comparing equivalent Xcc8004 populations on seeds, the presence
316 of *S. rhizophila* CFBP13503 negatively impacted the population of Xcc8004 on germinated
317 seeds compared to the mutant strain lacking the T6SS gene *hcp*. This highlights the potential
318 role of T6SS during the early interactions between bacteria. The effects of *S. rhizophila*
319 CFBP13503 T6SS persist overtime at the seedling stage, as a lower population of Xcc is
320 observed in the presence of the wild-type strain. Since Xcc8004 is a seed-borne pathogen,
321 limiting its transmission to the seedling stage appears to be a promising strategy for managing
322 this pathogen. However, further studies are needed on host plants to assess whether the T6SS
323 of *S. rhizophila* CFBP13503 can limit the pathogenicity of Xcc8004 by reducing its population
324 size.

325 It is also noteworthy that the presence or absence of T6SS, as well as its mutation, does not
326 impact the transmission of *S. rhizophila* CFBP13503 when in competition with Xcc8004.
327 Consequently, the T6SS of *S. rhizophila* CFBP13503 does not seem to be involved in its
328 adhesion or colonization capacities of radish seed and seedling, unlike what has been observed
329 in other bacterial species (Cassan et al., 2021; Mosquito et al., 2019).

330 *S. rhizophila* CFBP13503 possesses seven VgrG proteins, each of which is associated with a
331 chaperone protein and a putative effector. This diversity of VgrG proteins may allow for various
332 associations in the arrangement of VgrG trimers, enhancing the versatility of the T6SS.

333 Additionally, *S. rhizophila* CFBP13503 has five PAAR-domains containing protein. The
334 presence of PAAR proteins sharpens the tip of the VgrG trimer, creating opportunities for
335 different toxic effector associations during each firing event. Two of these PAAR proteins
336 possess a C-terminal toxic domain related to DNase activity. The extensive repertoire of
337 effectors identified in *S. rhizophila* CFBP13503 includes Tle1-type phospholipases (Flaughnatti
338 et al., 2016; Russell et al., 2013) capable of lysing the membranes of target bacteria, DNases
339 (Tde) that exhibit antibacterial properties by targeting nucleic acids, amidases (Tae) that
340 degrade peptidoglycan to lyse the target bacterium, and potentially a pore-forming effector that
341 inhibits the growth of target cells by depolarizing the inner membrane. Furthermore, there are
342 other effectors whose activities have yet to be discovered. These effectors are predicted to target
343 different components of bacterial cells, contributing to the antibacterial phenotype against
344 Xcc8004. Interestingly, some components and effectors in *S. rhizophila* CFBP13503 could also
345 exhibit anti-eukaryotic activity. For example, the DUF2345 domain of VgrG has been shown
346 to intoxicate yeast, as demonstrated by *Klebsiella pneumoniae* VgrG4 (Storey et al., 2020).
347 Moreover, the two "evolved" PAAR proteins, which contain a C-terminal Ntox15 domain,
348 share a significant identity (>30%) with the DNase effector TafE of *Acinetobacter baumannii*
349 strain 17978, known for its involvement in yeast killing (Luo et al., 2023). Some Tle effectors
350 were also shown to target bacteria and eukaryotic cells (Jiang et al., 2014; Jiang et al., 2016).
351 The combination of these diverse effectors, either individually or in synergy (LaCourse et al.,
352 2018), likely contributes to the competitive advantage of *S. rhizophila* CFBP13503 over Xcc *in*
353 *vitro*. Despite possessing only one T6SS, the diverse repertoire of effectors enables *S. rhizophila*
354 CFBP13503 to effectively combat bacterial competitors and potentially exert antibacterial
355 effects against Xcc8004.

356 Type VI secretion system is not frequently found in *Stenotrophomonas* genomes. Less than
357 10% of the genome sequences analyzed possessed a T6SS genetic cluster, which is generally
358 presented in a single copy. This frequency is relatively low compared with other bacterial
359 genera of the *Lysobacterales* where T6SS is present in approximately 50% of sequenced strains
360 (Bayer-Santos et al., 2019). A novel subgroup 3 within *Lysobacterales*, exclusively associated
361 with *Stenotrophomonas* species, was revealed by TssC-based phylogeny analysis. Notably, this
362 subgroup was not identified in the previous study conducted by Bayer-Santos et al. (2019) on
363 T6SS classification within *Lysobacterales*. Consistent with their findings, our analysis also
364 identified *Stenotrophomonas* T6SS classified into both group i1 and group i4. However, group
365 i4 T6SS appears to be more prevalent within the *Stenotrophomonas* genus. This is the case for
366 the T6SS of *S. rhizophila* CFBP13503 and more generally for strains affiliated with the *S.*
367 *rhizophila* complex, including the type strain DSM14405^T (Wolf et al., 2002). *S. rhizophila*
368 strains are not only known for their ability to colonize a wide range of plant species following
369 seed inoculation (Schmidt et al., 2012; Simonin et al., 2023) but also to exhibit antifungal (Berg
370 and Ballin, 1994) and antibacterial activities (Lottmann et al., 1999). For instance, the strain *S.*
371 *rhizophila* DSM14405^T protects plants against *Fusarium solani* and displays antagonistic
372 activity against various phytopathogenic fungi under high salt conditions (Egamberdieva et al.,
373 2011). Interestingly some T6SS genes of *S. rhizophila* DSM14405^T are strongly up-regulated
374 in response to osmotic stress (Alavi et al., 2013; Liu et al., 2022). More available genomes from
375 the *S. rhizophila* complex will confirm later the T6SS uniformity in these species. Nevertheless,

376 the large range of putative T6SS effectors in CFBP 13503 reinforces the interest in *S. rhizophila*
377 antimicrobial activities.

378 The T6SS of *S. rhizophila* CFBP13503 plays a crucial role in its antibiosis against Xcc8004
379 and in limiting Xcc8004 transmission from radish seed to seedling, highlighting its potential in
380 biocontrol of seed-borne pathogenic bacteria. The T6SS has emerged as a powerful tool in
381 biocontrol strategies, offering a novel approach to combat plant pathogens. However, further
382 research is necessary to fully understand its impact within complex microbial ecosystems. By
383 investigating the role of the T6SS in diverse bacterial communities, valuable insights can be
384 gained regarding its functionality, interactions with other microorganisms, and ecological
385 consequences. Understanding the influence of the T6SS on complex bacterial communities is
386 essential for unlocking its full potential and maximizing its contribution to biocontrol
387 approaches.

388

389 **4- EXPERIMENTAL PROCEDURES**

390 **Bacterial strains and growth conditions**

391 Bacterial strains and plasmids used in this study are listed in Table S1. *Stenotrophomonas*
392 *rhizophila* CFBP13503 and Xcc 8004::GUS-GFP (Cerutti et al., 2017) were grown at 28°C on
393 tryptic soy agar 1/10 strength (TSA10: 17 g.l-1 tryptone, 3 g.l-1 soybean peptone, 2.5 g.l-1
394 glucose, 5 g.l-1 NaCl, 5 g.l-1 K2HPO4, and 15 g.l-1 agar) or tryptic soy broth 1/10 strength
395 (TSB10). *E. coli* DH5α and *E. coli* MFDpir (Ferrières et al., 2010) were grown at 37°C on
396 Luria-Bertani (LB 10 g.l-1 tryptone, 5 g.l-1 Yeast extract, 10 g.l-1 NaCl) medium. LB medium
397 was supplemented with 0.3mM 2,5-diaminopimelic acid (Fisher Scientific, UK) for
398 auxotrophic *E. coli* MFDpir.

399

400 **Construction of *S. rhizophila* CFBP13503Δ*hcp* and CFBP13503Δ*tssB* and their**

401 complementation

402 Unmarked *hcp* (HKJBHOBG_02305) and *tssB* (HKJBHOBG_02307) deletions were
403 performed by allelic exchange using the suicide vector pEX18Tc (Hoang et al. 1998). The
404 deletion plasmids pEX18Tc-Δ*hcp* and pEX18Tc-Δ*tssB* were constructed using the TEDA
405 cloning procedure (Xia et al., 2019). Briefly, pEX18Tc was digested with *Xba*I (New England
406 Biolabs, France) followed by a dephosphorylation step using the shrimp alkaline phosphatase
407 (Phusion High-fidelity DNA polymerase, New England Biolabs, France). *hcp* and *tssB* flanking
408 regions were PCR-amplified from CFBP13503 with the Phusion High-Fidelity DNA
409 polymerase (New England Biolabs, France), and the primer pairs listed in Table S2. The
410 dephosphorylated pEX18Tc vector and PCR products were purified using the NucleoSpin Gel
411 and PCR Clean-up kit (Macherey-Nagel, Düren, Germany). TEDA reaction was then carried
412 out by mixing 150 ng of pEX18Tc with the corresponding PCR products at a molar ratio of 1:4.
413 One hundred μL of *E. coli* DH5α were transformed with 5 μL of TEDA reaction using the Inoue
414 transformation procedure (Sambrook and Russell, 2006) modified by Xia et al. (2019).
415 Amplicon insertions were validated by colony PCR with the primer pair M13F/M13R. Plasmids
416 (pEX18Tc-Δ*hcp*) were extracted with the NucleoSpin plasmid kit (Macherey-Nagel, Düren,
417 Germany), and insertion regions were verified by sequencing (Azenta Life Sciences, Germany).
418 *E. coli* MFDpir was transformed with pEX18Tc-Δ*hcp* and pEX18Tc-Δ*tssB* using the modified
419 Inoue method. Plasmids were transferred to *S. rhizophila* CFBP13503 via conjugation. *S.*
420 *rhizophila* CFBP13503 transconjugants were selected on TSA10 supplemented with
421 tetracycline (20 μg/mL). The resulting colonies were grown in TSB10 (28°C, 120 rpm, 3h) and
422 bacterial suspensions were spread on TSA10 supplemented with 5% saccharose. Allelic
423 exchanges were validated by PCR and sequencing.

424 Deletion mutants were complemented by allele exchange. Briefly, *hcp* and *tssB* were
425 PCR-amplified with the primer pairs Hcp-pEX18-UpF/Hcp-pEX18-DnR and TssB-pEX18-
426 UcpF/TssB-pEX18-DnR (Table S2). TEDA reactions were performed at a vector: insert molar
427 ratio of 1:1. pEX18Tc-*hcp* and pEX18Tc-*tssB* were transferred by electroporation to
428 CFBP13503Δ*hcp* and CFBP13503Δ*tssB*, respectively. To carry out this electroporation step,
429 bacteria were grown in TSA to OD₆₀₀ of 0.5-0.7. Bacterial cultures were centrifuged (4100 g,

430 10 min, 2°C), and pellets were washed four times in cold sterile water, once in 10% glycerol
431 and finally resuspended in 10% glucose before storage at -80°C. CFBP13503 Δ hcp and
432 CFBP13503 Δ tssB were transformed with 150 ng of pEX18Tc-hcp and pEX18Tc-tssB (2kV,
433 5ms). Transformants were selected on TSA10 supplemented with tetracycline (20 μ g/mL). The
434 resulting colonies were grown in TSB10 (28°C, 120 rpm, 3h) and bacterial suspensions were
435 spread on TSA10 supplemented with 5% saccharose. Allelic exchanges were validated by PCR
436 and sequencing.

437

438 ***In vitro* confrontation assays**

439 *S. rhizophila* CFBP13503, the isogenic T6SS-deficient mutants, the complemented T6SS
440 mutants and Xcc8004-Rif^R were cultured overnight in 10 mL of TSB10 (28°C, 150 rpm).
441 Cultures were centrifuged (4,000 g, 8 min, 20°C) and the resulting pellets were resuspended in
442 sterile water. Bacterial suspensions were calibrated to OD₆₀₀ of 0.5 (~10⁹ cells.mL⁻¹). For
443 confrontation on a solid medium, calibrated suspensions were mixed at a ratio of 1:1 (i.e. 100 μ L
444 of each strain). Single suspensions were prepared as a control by mixing 100 μ L of bacterial
445 cultures with 100 μ L of sterile water. Drops of 20 μ l were deposited on TSA10, dried for 15
446 minutes under a laminar and incubated at 28°C for 6 and 24 h. At each incubation time, cells
447 were resuspended in 2.5 mL of sterile water, serial-diluted and plated on TSA10 supplemented
448 with 50 μ g/mL of rifampicin (selection of Xcc8004-Rif^R) or with 50 μ g/mL of spectinomycin
449 and 100 μ g/mL of ampicillin (selection of *S. rhizophila* strains). For confrontation in liquid
450 medium, calibrated suspensions were mixed at a ratio of 1:1 (i.e. 500 μ L of each strain in 9 mL
451 TSB10). As a control, single-strain suspensions were prepared by mixing 500 μ L of bacterial
452 cultures with 500 μ l of TSB10. The confrontations were incubated at 28°C 150 rpm for 6 and
453 24h. At each incubation time, confrontations were serial-diluted and plated on TSA10
454 supplemented with 50 μ g/mL of rifampicin (selection of Xcc8004-Rif^R) or with 50 μ g/mL of
455 spectinomycin and 100 μ g/mL of ampicillin (selection of *S. rhizophila* strains).

456

457 ***In planta* transmission assays**

458 Three subsamples of 300 radish seeds (*Raphanus sativus* var. Flamboyant 5) were surface
459 sterilized using the protocol described in Simonin et al. (2023). Sterilized seeds were dried 30
460 min before inoculation under a laminar. Bacterial suspensions were prepared at an OD₆₀₀ of 0.5
461 from 24h bacterial mats on TSA10. These suspensions corresponded to (i) Xcc8004, (ii)
462 Xcc8004/CFBP13503 (1:1 ratio) and (iii) Xcc8004/CFBP13503 Δ hcp (1:1 ratio). Seeds were
463 either soaked into bacterial suspensions (15 min, 20°C, 70 rpm) or sterile water (non-inoculated
464 condition). Seeds were dried for 15 min on sterile paper under a laminar. Inoculated and non-
465 inoculated seeds were placed on sterile folded moistened papers in sterile plastic boxes. Three
466 repetitions (20 seeds per repetition) were carried out per condition. Boxes were incubated in a
467 growth chamber (photoperiod: 16h/8h, temperature 20°C). Germinated seeds were collected 24
468 h post-inoculation (n=3, 20 germinated seeds per repetition). Seedlings were harvested five
469 days post-inoculation (n=3, 20 seedlings per repetition). The same experiment was repeated
470 with n=4 repetitions. Bacterial population sizes were assessed by dilution and plating on TSA10

471 supplemented with appropriate antibiotics (see *in vitro* confrontation assays). Seed-associated
472 bacteria were recovered 15 min after inoculation (initial time) by vortexing 20 seed pools in 2
473 mL of sterile water for 30 seconds. Germinated seeds (20 seedling pools) were grounded in 4
474 mL of sterile water. The entire aerial and root parts of seedlings (20 seedling pools) including
475 both endophytic and epiphytic bacteria were separated and grounded in 4 mL of sterile water.
476 No bacterial growth was observed on the selective media for the non-inoculated seeds,
477 germinated seeds and seedlings attesting the absence of culturable bacteria in the control.

478

479 **Genomic analysis of *S. rhizophila* CFBP13503 T6SS and effector prediction**

480 The genomic sequence of *S. rhizophila* CFBP13503 (SAMN09062466) was initially obtained
481 through paired-end Illumina sequencing (Torres-Cortés et al., 2019). To circularize the genomic
482 sequence of CFBP13503, PacBio sequencing was performed on an RS2 machine (Genotoul,
483 Castanet-Tolosan, France). PacBio reads were filtered and demultiplexed using the ccs v6.3.0
484 and lima v2.5.1 tools of the PacBio SMRT Tools v11.0.0.146107 toolkit and then assembled
485 and circularized using Flye v2.9 (Kolmogorov et al., 2019). The sequence start was fixed using
486 the fixstart option of Circlator v1.5.1 (Hunt et al., 2015). Polishing with PacBio reads was
487 performed using Flye v2.9 (Kolmogorov et al., 2019). Polishing with Illumina HiSeq3000 short
488 reads was done using Pilon v1.24 (Walker et al., 2014) with the setting --mindepth 0. Genome
489 annotation was performed with Prokka v1.14.6 (Seemann, 2014).

490 T6SS components were identified by conducting NCBI BLASTP analysis on protein
491 sequences. Effector-immunity encoding gene pairs and chaperones were identified by analyzing
492 genes downstream of *vgrG* and PAAR motif-containing genes. The conserved domain database
493 of the NCBI was used to identify T6SS-related conserved domains. Structural homology-based
494 searches were made using Alphafold2 (Jumper et al., 2021) structure prediction of putative
495 effectors followed by a DALI (Holm et al., 2023) search analysis or using the Foldseek search
496 server (van Kempen et al., 2023).

497

498 **Phylogenetic analysis of T6SS**

499 A total of 991 genome sequences of *Stenotrophomonas* were downloaded from the NCBI.
500 Genomes with fewer than 10 markers (Marker_lineage = f_Xanthomonadaceae) absent or in
501 multicity (CheckM v1.1.6; Parks et al., 2015) were conserved for further analysis. A multi-
502 locus species tree was created with Automlst (Alanjary et al., 2019). Non-*Stenotrophomonas*-
503 affiliated genomes were excluded from further analysis, resulting in a final dataset comprising
504 835 *Stenotrophomonas* genomes. Sequence relatedness between the selected 835 genomes
505 sequences was assessed with KI-S (Briand et al., 2021) using 50% of shared 15-mers, a proxy
506 for delineating bacterial species. Genome sequences were annotated with Prokka 1.14.6
507 (Seemann, 2014). The presence of T6SS genomic clusters was predicted with MacSyFinder2
508 (Néron et al., 2023). TssC protein sequences were retrieved following BLASTp searches using
509 TssC sequences of *Stenotrophomonas rhizophila* CFBP13503 (iT6SS group 4b) and
510 *Stenotrophomonas* sp. LM091 (iT6SS group 1). BLASTp hits with >25% identity over 75% of

511 protein length were conserved. TssC sequences were aligned using MUSCLE. A Kimura two-
512 parameter neighbor-joining tree was constructed with 1000 bootstraps with SeaView v4.7
513 (Gouy et al., 2010). The T6SS groups have been assigned according to the previously defined
514 nomenclatures (Bayer-Santos et al., 2019; Bernal et al., 2017; Gallegos-Monterrosa and
515 Coulthurst, 2021).

516

517 **ACKNOWLEDGEMENTS**

518 This work was funded by the TypeSEEDS project (INRAE: Plant Health and Environment
519 division, HoloFlux Metaprogram) and the Region des Pays de la Loire (RFI “Objectif
520 Végétal”). We thank the CIRM-CFBP for providing access to strains of their culture collection.

521

522 **CONFLICT OF INTEREST STATEMENT**

523 The authors declare that they have no conflicts of interest.

524

525 **DATA AVAILABILITY STATEMENT**

526 *Sequence data generated during this work can be found in the GenBank database. The coding*
527 *sequence of CFBP13503 has been deposited in GenBank under accession number CP128598.*

528

529

530 **REFERENCES**

531 Alanjary, M., Steinke, K. & Ziemert, N. (2019) AutoMLST: an automated web server for
532 generating multi-locus species trees highlighting natural product potential. *Nucleic Acids
533 Research*, 47, W276–W282.

534

535 Alavi, P., Starcher, M., Zachow, C., Mueller, H. & Berg, G. (2013) Root-microbe systems: the
536 effect and mode of interaction of Stress Protecting Agent (SPA) *Stenotrophomonas rhizophila*
537 DSM14405T. *Frontiers in Plant Science*, 4, 141.

538

539 Baker, K.F. & Smith, S.H. (1966) Dynamics of seed transmission of plant pathogens. *Annual
540 Review of Phytopathology*, 4, 311–332.

541

542 Barret, M., Guimbaud, J., Darrasse, A. & Jacques, M. (2016) Plant microbiota affects seed
543 transmission of phytopathogenic microorganisms. *Molecular Plant Pathology*, 17, 791–795.

544

545 Bayer-Santos, E., Ceseti, L. de M., Farah, C.S. & Alvarez-Martinez, C.E. (2019) Distribution,
546 function and regulation of type 6 secretion systems of *Xanthomonadales*. *Frontiers in
547 Microbiology*, 10:1635.

548

549 Berg, G. & Ballin, G. (1994) Bacterial Antagonists to *Verticillium dahliae* Kleb. *Journal of
550 Phytopathology*, 141, 99–110.

551

552 Berg, G., Marten, P. & Ballin, G. (1996) *Stenotrophomonas maltophilia* in the rhizosphere of
553 oilseed rape — occurrence, characterization and interaction with phytopathogenic fungi.
554 *Microbiological Research*, 151, 19–27.

555

556 Bernal, P., Allsopp, L.P., Filloux, A. & Llamas, M.A. (2017) The *Pseudomonas putida* T6SS
557 is a plant warden against phytopathogens. *The ISME Journal*, 11, 972–987.

558

559 Bernal, P., Llamas, M.A. & Filloux, A. (2018) Type VI secretion systems in plant-associated
560 bacteria. *Environmental Microbiology*, 20, 1–15.

561

562 Berni, B., Soscia, C., Djermoun, S., Ize, B. & Bleves, S. (2019) A type VIsecretion system
563 trans-kingdom effector is required for the delivery of a novel antibacterial toxin in
564 *Pseudomonas aeruginosa*. *Frontiers in Microbiology*, 10.

565

566 Briand, M., Bouzid, M., Hunault, G., Legeay, M., Fischer-Le Saux, M. & Barret, M. (2021) A
567 rapid and simple method for assessing and representing genome sequence relatedness. *Peer
568 Community Journal*, 1.

569

570 Cassan, F.D., Coniglio, A., Amavizca, E., Maroniche, G., Cascales, E., Bashan, Y., et al. (2021)
571 The *Azospirillum brasilense* type VI secretion system promotes cell aggregation, biocontrol
572 protection against phytopathogens and attachment to the microalgae *Chlorella sorokiniana*.
573 *Environmental Microbiology*, 23, 6257–6274.

574 Cerutti, A., Jauneau, A., Auriac, M.-C., Lauber, E., Martinez, Y., Chiarenza, S., et al. (2017)
575 Immunity at cauliflower hydathodes controls systemic infection by *Xanthomonas campestris*
576 *pv campestris*. *Plant Physiology*, 174, 700–716.

577

578 Chen, W.-J., Kuo, T.-Y., Hsieh, F.-C., Chen, P.-Y., Wang, C.-S., Shih, Y.-L., et al. (2016)
579 Involvement of type VI secretion system in secretion of iron chelator pyoverdine in
580 *Pseudomonas taiwanensis*. *Scientific Reports*, 6, 1–14.

581 Cherrak, Y., Flaugnatti, N., Durand, E., Journet, L. & Cascales, E. (2019) Structure and activity
582 of the type VI secretion system. *Microbiology Spectrum*, 7(4).

583

584 Chesneau, G., Laroche, B., Préveaux, A., Marais, C., Briand, M., Marolleau, B., et al. (2022)
585 Single seed microbiota: assembly and transmission from parent plant to seedling. *mBio*, 13,
586 e01648-22.

587

588 Choi, Y., Kim, N., Manna, M., Kim, H., Park, J., Jung, H., et al. (2020) Characterization of
589 type VI secretion system in *Xanthomonas oryzae* pv. *oryzae* and its role in virulence to rice.
590 *The Plant Pathology Journal*, 36, 289–296.

591

592 Cianfanelli, F.R., Diniz, J.A., Guo, M., Cesare, V.D., Trost, M. & Coulthurst, S.J. (2016) VgrG
593 and PAAR proteins define distinct versions of a functional type VI secretion system. *PLOS*
594 *Pathogens*, 12, e1005735.

595

596 Darrasse, A., Darsonval, A., Boureau, T., Brisset, M.-N., Durand, K. & Jacques, M.-A. (2010)
597 Transmission of plant-pathogenic bacteria by nonhost seeds without induction of an associated
598 defense reaction at emergence. *Applied and Environmental Microbiology*, 76, 6787–6796.

599

600 Decoin, V., Barbey, C., Bergeau, D., Latour, X., Feuilloley, M.G., Orange, N., Merieau, A (2014). A type
601 VI secretion system is involved in *Pseudomonas fluorescens* bacterial competition. *PLoS One*.
602 9(2):e89411.

603

604 Denancé, N. & Grimault, V. (2022) Seed pathway for pest dissemination: The ISTA Reference
605 Pest List, a bibliographic resource in non-vegetable crops. *EPPO Bulletin*, 52, 434–445.

606 Egamberdieva, D., Kucharova, Z., Davranov, K., Berg, G., Makarova, N., Azarova, T., et al.
607 (2011) Bacteria able to control foot and root rot and to promote growth of cucumber in salinated
608 soils. *Biology and Fertility of Soils*, 47, 197–205.

609

610 Engering, A., Hogerwerf, L. & Slingenbergh, J. (2013) Pathogen-host-environment interplay
611 and disease emergence. *Emerging Microbes & Infections*, 2, e5.

612

613 Fei, N., Ji, W., Yang, L., Yu, C., Qiao, P., Yan, J., Guan W, Yang, Y., Zhao, T. (2022) Hcp of the type VI
614 secretion system (T6SS) in *Acidovorax citrulli* group II strain Aac5 has a dual role as a core structural
615 protein and an effector protein in colonization, growth ability, competition, biofilm formation, and
616 ferric iron absorption. *Int J Mol Sci.* Aug 25;23(17):9632.

617

618 Ferrières, L., Hémery, G., Nham, T., Guérout, A.-M., Mazel, D., Beloin, C., et al. (2010) Silent
619 mischief: bacteriophage Mu insertions contaminate products of *Escherichia coli* random
620 mutagenesis performed using suicidal transposon delivery plasmids mobilized by broad-host-
621 range RP4 conjugative machinery. *Journal of Bacteriology*, 192, 6418–6427.
622

623 Flaugnatti, N., Le, T.T.H., Canaan, S., Aschtgen, M.-S., Nguyen, V.S., Blangy, S., et al. (2016)
624 A phospholipase A1 antibacterial Type VI secretion effector interacts directly with the C-
625 terminal domain of the VgrG spike protein for delivery. *Molecular Microbiology*, 99, 1099–
626 1118.
627

628 Flaugnatti, N., Rapisarda, C., Rey, M., Beauvois, S.G., Nguyen, V.A., Canaan, S., et al. (2020)
629 Structural basis for loading and inhibition of a bacterial T6SS phospholipase effector by the
630 VgrG spike. *The EMBO Journal*, 39, e104129.
631

632 Gallegos-Monterrosa, R. & Coulthurst, S.J. (2021) The ecological impact of a bacterial weapon:
633 microbial interactions and the type VI secretion system. *FEMS microbiology reviews*, 45,
634 fuab033.
635

636 Gouy, M., Guindon, S. & Gascuel, O. (2010) SeaView version 4: a multiplatform graphical
637 user interface for sequence alignment and phylogenetic tree building. *Molecular Biology and*
638 *Evolution*, 27, 221–224.
639

640 Granato, E.T., Meiller-Legrand, T.A. & Foster, K.R. (2019) The evolution and ecology of
641 bacterial warfare. *Current Biology*, 29, R521–R537.
642

643 Gröschel, M.I., Meehan, C.J., Barilar, I., Diricks, M., Gonzaga, A., Steglich, M., et al. (2020)
644 The phylogenetic landscape and nosocomial spread of the multidrug-resistant opportunist
645 *Stenotrophomonas maltophilia*. *Nature Communications*, 11, 2044.
646

647 Hersch, S.J., Manera, K. & Dong, T.G. (2020) Defending against the Type Six Secretion
648 System: beyond Immunity Genes. *Cell Reports*, 33, 10-13.
649

650 Ho, B.T., Dong, T.G. & Mekalanos, J.J. (2014) A view to kill: the bacterial type VI secretion
651 system. *Cell Host & Microbe*, 15, 9–21.
652

653 Holm, L., Laiho, A., Törönen, P. & Salgado, M. (2023) DALI shines a light on remote
654 homologs: One hundred discoveries. *Protein Science*, 32, e4519.
655

656 Hunt, M., Silva, N.D., Otto, T.D., Parkhill, J., Keane, J.A. & Harris, S.R. (2015) Circlator:
657 automated circularization of genome assemblies using long sequencing reads. *Genome Biology*,
658 16, 294.
659

660 Jacques, M.-A., Arlat, M., Boulanger, A., Boureau, T., Carrère, S., Cesbron, S., et al. (2016)
661 Using ecology, physiology, and genomics to understand host specificity in *Xanthomonas*.
662 *Annual Review of Phytopathology*, 54, 163–187.

663

664 Jiang, F., Wang, X., Wang, B., Chen, L., Zhao, Z., Waterfield, N.R., et al. (2016) The
665 *Pseudomonas aeruginosa* type VI secretion PGAP1-like effector induces host autophagy by
666 activating endoplasmic reticulum stress. *Cell Reports*, 16, 1502–1509.

667

668 Jiang, F., Waterfield, N.R., Yang, J., Yang, G. & Jin, Q. (2014) A *Pseudomonas aeruginosa*
669 type VI secretion phospholipase D effector targets both prokaryotic and eukaryotic cells. *Cell*
670 *Host & Microbe*, 15, 600–610.

671

672 Jumper, J., Evans, R., Pritzel, A., Green, T., Figurnov, M., Ronneberger, O., et al. (2021) Highly
673 accurate protein structure prediction with AlphaFold. *Nature*, 596, 583–589.

674

675 Jurénas, D. & Journet, L. (2021) Activity, delivery, and diversity of type VI secretion effectors.
676 *Molecular Microbiology*, 115, 383–394.

677

678 Kempen, M. van, Kim, S.S., Tumescheit, C., Mirdita, M., Lee, J., Gilchrist, C.L.M., et al.
679 (2023) Fast and accurate protein structure search with Foldseek. *Nature Biotechnology*, 1–4.

680 Kolmogorov, M., Yuan, J., Lin, Y. & Pevzner, P.A. (2019) Assembly of long, error-prone reads
681 using repeat graphs. *Nature Biotechnology*, 37, 540–546.

682

683 LaCourse, K.D., Peterson, S.B., Kulasekara, H.D., Radey, M.C., Kim, J. & Mougous, J.D.
684 (2018) Conditional toxicity and synergy drive diversity among antibacterial effectors. *Nature*
685 *Microbiology*, 3.

686 Lien, Y.-W. & Lai, E.-M. (2017) Type VI secretion effectors: methodologies and biology.
687 *Frontiers in Cellular and Infection Microbiology*, 7.

688

689 Lin, J., Zhang, W., Cheng, J., Yang, X., Zhu, K., Wang, Y., et al. (2017) A *Pseudomonas* T6SS
690 effector recruits PQS-containing outer membrane vesicles for iron acquisition. *Nature*
691 *Communications*, 8, 14888.

692

693 Lin, J.-S., Pissaridou, P., Wu, H.-H., Tsai, M.-D., Filloux, A. & Lai, E.-M. (2018) TagF-
694 mediated repression of bacterial type VI secretion systems involves a direct interaction with the
695 cytoplasmic protein Fha. *Journal of Biological Chemistry*, 293, 8829–8842.

696

697 Lin, L., Capozzoli, R., Ferrand, A., Plum, M., Vettiger, A. & Basler, M. (2022). Subcellular
698 localization of Type VI secretion system assembly in response to cell-cell contact. *EMBO*
699 *Journal*, 41(13):e108595.

700

701

702

703

704 Liu, Y., Gao, J., Wang, N., Li, X., Fang, N. & Zhuang, X. (2022) Diffusible signal factor
705 enhances the saline-alkaline resistance and rhizosphere colonization of *Stenotrophomonas*
706 *rhizophila* by coordinating optimal metabolism. *Science of The Total Environment*, 834,
707 155403.

708

709 Liyanapathiranage, P., Jones, J.B. & Potnis, N. (2021) A mutation of a single core gene, tssM,
710 of Type VI secretion system of *Xanthomonas perforans* influences virulence, epiphytic survival
711 and transmission during pathogenesis on tomato. *Phytopathology*, 112, 752– 764.

712

713 Lopez, J., Le, N.H., Moon, K.H., Salomon, D., Bosis, E. & Feldman, M.F. (2021)
714 Formylglycine-generating enzyme-like proteins constitute a novel family of widespread Type
715 VI secretion system immunity proteins. *Journal of bacteriology*, 203:e00281-21.

716

717 Lottmann, J., Heuer, H., Smalla, K. & Berg, G. (1999) Influence of transgenic T4-lysozyme-
718 producing potato plants on potentially beneficial plant-associated bacteria. *FEMS Microbiology
719 Ecology*, 29, 365–377.

720

721 Luo, J., Chu, X., Jie, J., Sun, Y., Guan, Q., Li, D., et al. (2023) *Acinetobacter baumannii* kills
722 fungi via a type VI DNase effector. *mBio*, 14:e03420–03422.

723

724 Ma, L.-S., Hachani, A., Lin, J.-S., Filloux, A. & Lai, E.-M. (2014) *Agrobacterium tumefaciens*
725 deploys a superfamily of type VI secretion DNase effectors as weapons for interbacterial
726 competition in planta. *Cell Host & Microbe*, 16, 94–104.

727

728 Minkwitz, A. & Berg, G. (2001) Comparison of antifungal activities and 16S ribosomal DNA
729 sequences of clinical and environmental isolates of *Stenotrophomonas maltophilia*. *Journal of
730 Clinical Microbiology*, 39, 139–145.

731

732 Miyata, S.T., Unterweger, D., Rudko, S.P. & Pukatzki, S. (2013) Dual expression profile of
733 type VI secretion system immunity genes protects pandemic *Vibrio cholerae*. *PLOS Pathogens*,
734 9, e1003752.

735

736 Montenegro Benavides, N.A., Alvarez B, A., Arrieta-Ortiz, M.L., Rodriguez-R, L.M., Botero,
737 D., Tabima, J.F., et al. (2021) The type VI secretion system of *Xanthomonas phaseoli* pv.
738 *manihotis* is involved in virulence and in vitro motility. *BMC microbiology*, 21, 14.

739

740 Mosquito, S., Bertani, I., Licastro, D., Compani, S., Myers, M.P., Hinarejos, E., et al. (2019) In
741 planta colonization and role of T6SS in two rice *Kosakonia* endophytes. *Molecular Plant-
742 Microbe Interactions*®, 33, 349–363.

743

744 Néron, B., Denise, R., Coluzzi, C., Touchon, M., Rocha, E.P.C. & Abby, S.S. (2023)
745 MacSyFinder v2: Improved modelling and search engine to identify molecular systems in
746 genomes. *Peer Community Journal*, 3.

747

748 Newcombe, G., Harding, A., Ridout, M. & Busby, P.E. (2018) A hypothetical bottleneck in the
749 plant microbiome. *Frontiers in Microbiology*, 9.

750

751 Parks, D.H., Imelfort, M., Skennerton, C.T., Hugenholtz, P. & Tyson, G.W. (2015) CheckM:
752 assessing the quality of microbial genomes recovered from isolates, single cells, and
753 metagenomes. *Genome Research*, 25, 1043–1055.

754 Randhawa, P. (1984) Selective isolation of *Xanthomonas campestris* pv. *campestris* from
755 Crucifer seeds. *Phytopathology*, 74.

756

757 Rezki, S., Campion, C., Iacomi-Vasilescu, B., Preveaux, A., Toualbia, Y., Bonneau, S., et al.
758 (2016) Differences in stability of seed-associated microbial assemblages in response to invasion
759 by phytopathogenic microorganisms. *PeerJ*, 4, e1923.

760

761 Rezki, S., Campion, C., Simoneau, P., Jacques, M.-A., Shade, A. & Barret, M. (2018) Assembly
762 of seed-associated microbial communities within and across successive plant generations. *Plant
763 and Soil*, 422, 67–79.

764

765 Russell, A.B., LeRoux, M., Hathazi, K., Agnello, D.M., Ishikawa, T., Wiggins, P.A., et al.
766 (2013) Diverse type VI secretion phospholipases are functionally plastic antibacterial effectors.
767 *Nature*, 496, 508–512.

768

769 Sambrook, J. & Russell, D.W. (2006) The Inoue method for preparation and transformation of
770 competent *E. coli*: “Ultra-competent” cells. *Cold Spring Harbor Protocols*, 2006,
771 pdb.prot3944.

772

773 Schmidt, C.S., Alavi, M., Cardinale, M., Müller, H. & Berg, G. (2012) *Stenotrophomonas
774 rhizophila* DSM14405T promotes plant growth probably by altering fungal communities in the
775 rhizosphere. *Biology and Fertility of Soils*, 48, 947–960.

776

777 Seemann, T. (2014) Prokka: rapid prokaryotic genome annotation. *Bioinformatics (Oxford,
778 England)*, 30, 2068–2069.

779

780 Shyntum, D.Y., Theron, J., Venter, S.N., Moleleki, L.N., Toth, I.K. & Coutinho, T.A. (2015)
781 *Pantoea ananatis* utilizes a type VI secretion system for pathogenesis and bacterial competition.
782 *Molecular Plant-Microbe Interactions*, 28, 420–431.

783

784 Si, M., Zhao, C., Burkinshaw, B., Zhang, B., Wei, D., Wang, Y., et al. (2017) Manganese
785 scavenging and oxidative stress response mediated by type VI secretion system in *Burkholderia
786 thailandensis*. *Proceedings of the National Academy of Sciences of the United States of
787 America*, 114, E2233–E2242.

788

789 Simonin, M., Briand, M., Chesneau, G., Rochefort, A., Marais, C., Sarniguet, A., et al. (2022)
790 Seed microbiota revealed by a large-scale meta-analysis including 50 plant species. *New
791 Phytologist*, 234, 1448–1463.

792 Simonin, M., Préveaux, A., Marais, C., Garin, T., Arnault, G., Sarniguet, A., et al. (2023)
793 Transmission of synthetic seed bacterial communities to radish seedlings: impact on microbiota
794 assembly and plant phenotype. *Peer Community Journal*, no. e95. doi : 10.24072/pcjournal.329.
795

796 Storey, D., McNally, A., Åstrand, M., Santos, J. sa-P.G., Rodriguez-Escudero, I., Elmore, B.,
797 et al. (2020) *Klebsiella pneumoniae* type VI secretion system-mediated microbial competition
798 is PhoPQ controlled and reactive oxygen species dependent. *PLOS Pathogens*, 16, e1007969.
799

800 Torres-Cortés, G., Garcia, B.J., Compant, S., Rezki, S., Jones, P., Préveaux, A., et al. (2019)
801 Differences in resource use lead to coexistence of seed-transmitted microbial populations.
802 *Scientific Reports*, 9, 1–13.
803

804 Trunk, K., Peltier, J., Liu, Y.-C., Dill, B.D., Walker, L., Gow, N.A.R., et al. (2018) The type
805 VI secretion system deploys antifungal effectors against microbial competitors. *Nature
806 Microbiology*, 3, 920–931.
807

808 Unterweger, D., Kostiuk, B. & Pukatzki, S. (2017) Adaptor proteins of type VI secretion system
809 effectors. *Trends in Microbiology*, 25, 8–10.
810

811 Vicente, J.G. & Holub, E.B. (2013) *Xanthomonas campestris* pv. *campestris* (cause of black rot
812 of crucifers) in the genomic era is still a worldwide threat to brassica crops. *Molecular Plant
813 Pathology*, 14, 2–18.

814 Walker, B.J., Abeel, T., Shea, T., Priest, M., Abouelliel, A., Sakthikumar, S., et al. (2014) Pilon:
815 an integrated tool for comprehensive microbial variant detection and genome assembly
816 improvement. *PLOS ONE*, 9, e112963.
817

818 Weber, B.S., Hennon, S.W., Wright, M.S., Scott, N.E., Berardinis, V. de, Foster, L.J., et al.
819 (2016) Genetic dissection of the type VI secretion system in *Acinetobacter* and identification
820 of a novel peptidoglycan hydrolase, Tagx, required for its biogenesis. *mBio*, 7.
821

822 Wolf, A., Fritze, A., Hagemann, M. & Berg, G. (2002) *Stenotrophomonas rhizophila* sp. nov.,
823 a novel plant-associated bacterium with antifungal properties. *International Journal of
824 Systematic and Evolutionary Microbiology*, 52, 1937–1944.
825

826 Wolf, J. van der, Kastelein, P., Silva Júnior, T.A.F. da, Lelis, F.V. & Zouwen, P. van der (2019)
827 Colonization of siliques and seeds of rapid cycling *Brassica oleracea* plants by *Xanthomonas
828 campestris* pv. *campestris* after spray-inoculation of flower clusters. *European Journal of Plant
829 Pathology*, 154, 445–461.

830 Xia, Y., Li, K., Li, J., Wang, T., Gu, L. & Xun, L. (2019) T5 exonuclease-dependent assembly
831 offers a low-cost method for efficient cloning and site-directed mutagenesis. *Nucleic Acids
832 Research*, 47, e15–e15.
833

834 Zhang, J., Guan, J., Wang, M., Li, G., Djordjevic, M., Tai, C., et al. (2022) SecReT6 update: a
835 comprehensive resource of bacterial Type VI Secretion Systems. *Science China Life Sciences*.

836 **SUPPORTING INFORMATION LEGENDS**

837 **Figure S1. T6SS distribution among *Stenotrophomonas* sp..** Interactive circle packing
838 representation of *Stenotrophomonas* sp. genomes (n=835). Overall genome relatedness was
839 assessed by comparing the percentage of shared 15-mers. Each dot represents a genome
840 sequence, color-coded based on the T6SS group. The genomes were grouped using two distinct
841 thresholds to assess species-specific relationships (0.5) and interspecies relationships (0.25).

842

843 **Figure S2. Clustering of *Stenotrophomonas* genome sequences.** Circle packing
844 representation of *Stenotrophomonas* sp. genomes (n=835). Overall genome relatedness was
845 assessed by comparing the percentage of shared 15-mers. Each dot represents a genome
846 sequence. The coloured dots represent the type strains of each described *Stenotrophomonas*
847 species. The genomes were grouped using two distinct thresholds to assess species-specific
848 relationships (0.5) and interspecies relationships (0.25).

849

850 **Figure S3. Dynamics of Xcc8004 and CFBP13503 populations in confrontation from 0h
851 to 48h.** Confrontation between Xcc8004 and i) *S. rhizophila* CFBP13503 wild-type, ii) T6SS-
852 deficient mutants Δhcp (a) and $\Delta tssB$ (b) in TSA10 medium for 6h, 24h and 48h. Colony-
853 forming units (CFU) of Xcc and CFBP13503 populations were quantified on TSA10
854 supplemented with rifampicin and ampicillin-streptomycin respectively. The averages \pm sd of
855 6 replicates are plotted. Statistical analyses were performed using Dunn's Multiple Comparison
856 Test (* p-value < 0,05; ** p-value <0,005; *** p-value < 0,0005; **** p-value < 0,00005).

857

858 **Figure S4. Bactericidal activity of *S. rhizophila* CFBP13503 against *X. campestris* pv.
859 *campestris* 8004 in liquid medium.** Confrontation between Xcc8004 and *S. rhizophila*
860 CFBP13503 wild-type, or T6SS-deficient mutants (Δhcp and $\Delta tssB$) in TSB10 (liquid medium)
861 for 6h and 24h. Colony-forming units (CFU) were quantified on TSA10 supplemented with
862 rifampicin. The averages \pm sd of 3 replicates are plotted. Statistical analyses were performed
863 using Dunn's Multiple Comparison Test (* p-value < 0.05).

864

865 **Table S1. Strains and plasmids used in this study**

866

867 **Table S2. Primers used for T6SS mutant constructions**

868

869

870

871